Unusual chromic behaviour of the solid supramolecular 3D polymers $[(Me_3Sn)_nFe(CN)_6]_\infty$ ($n = 3/4$)

Safaa Eldin H. Etaiw [a,*], Amany M.A. Ibrahim [b]

[a] *Department of Chemistry, Faculty of Science, Tanta University, Tanta, Egypt*
[b] *Department of Chemistry, Faculty of Science, Ain Shams University, Cairo, Egypt*

Abstract

The orange polymer tris-(trimethyltin)hexacyanoferrate(III) (1) undergoes irreversible colour changes, turning pale green, green, pale blue and blue under the effect of UV irradiation at 366 nm, or pressure for 5 h, or heating at 100°C under nitrogen or in open air for 40 h, while the white polymer tetrakis-(trimethyltin)hexacyanoferrate(II) (2) turns grey and finally deep violet under the effect of pressure or heating (ca. 160°C) for a long time (ca. 60 h). The properties of the resulting coloured complexes were investigated by IR, UV–visible, ESR, Mössbauer spectroscopy, elemental and thermal analysis, and magnetic susceptibility measurements, indicating partial transformation of iron(III) to iron(II) in 1 and iron(II) to iron(III) in 2 respectively and suggesting the formation of stable semiconducting polymeric complexes of blue colour (final product), resembling that of Prussian blue, retaining their identity to form three-dimensional networks via trimethyltin connecting units.

1. Introduction

Hexacyanide metal building blocks are linked together by organometallic connecting units (like R_3Sn^+) to provide an interesting new class of compounds with potentially useful properties. The most important class of these compounds is the 3D-coordination polymers which may, for example, afford zeolite-like materials with channels or cavities capable of oxidative and catalytic applications [1–3]. These channels are also capable of encapsulating different organic and organometallic compounds to yield materials with unusual properties [3–8].

The organotin(IV) or organolead(IV) hexacyanide polymers of transition metal ions of the type $[(R_3M)_nM^d(CN)_6]_\infty$ where R = alkyl or aryl, M = Sn or Pb and M^d = Fe or Co, represent a novel class of 3D-coordination polymers [8–10]. The structures of these polymers have been studied by Fischer and coworkers [8], where the cobalt derivatives with Me_3Sn^+ and Me_3Pb^+ were successfully subjected to single-crystal X-ray studies. The non-superimposable

3D networks of these two homologues involve $Me_3M(NC)_2$ units (M = Sn or Pb) of trigonal bipyramidal configuration and remarkably wide channels whose walls are internally coated with constituents of the lipophilic Me_3M groups. In contrast, the Fe(III) homologue 1 has not been subjected to single-crystal X-ray study since it is affected by electromagnetic radiation. In this study our goal has been to investigate the photo- and thermochemical behaviour of solid $[(Me_3Sn)_3Fe(CN)_6]_\infty$ and its polymeric homologue $[(Me_3Sn)_4Fe(CN)_6]_\infty$.

2. Experimental

2.1. Materials

The investigated trimethyltin hexacyanoferrate polymers 1 and 2 were prepared according to reported procedures [11]. An aqueous solution containing 2 mmol of potassium hexacyanoferrate (III or II) was added to a stirred aqueous solution of trimethyltin chloride (6 or 8 mmol) to form orange and very pale greenish-white precipitates respectively. The products formed were fil-

tered off using a Schlenk tube, washed with small portions of water and dried under vacuum. Additions and isolation of the polymers [(Me₃Sn)₃Fe(CN)₆]ₙ 1 and [(Me₃Sn)₄Fe(CN)₆]ₙ 2 formed were carried out in the dark under nitrogen atmosphere.

2.2. Methods and instrumentation

Thermal treatment of the solid polymers was carried out in the open air using a thermostatted oven and also under nitrogen atmosphere in the dark using a Schlenk tube in a vacuum system. Irradiation of the samples was carried out using a medium pressure mercury lamp (Emita VP-60 180 W) in a quartz cell in open air and under nitrogen atmosphere. A hydraulic press was used to press the polymers 1 and 2 at 5000 kg cm⁻² for 5 and 7 h respectively. The coloured products of polymer 1 are the pale green 1a, green 1b, pale blue 1c and dark blue 1d, and those of polymer 2 are the grey 2a, and violet 2b. IR spectra were recorded on a Perkin-Elmer 683 IR spectrophotometer (KBr technique). Microanalyses were carried out with a Perkin-Elmer 2400 automatic elemental analyzer, and metal analysis was carried out with a Perkin-Elmer 2380 atomic absorption spectrophotometer. X-ray powder diffraction patterns were recorded using a Phillips PW-1729 X-ray generator. ESR spectra were recorded at room temperature using a Jeol JEX-FE2XG spectrophotometer, DTA thermograms were recorded using a Dupont 970 thermal analyzer with 910 differential scanning calorimeter, while TGA was carried out with a Schimadzu AT50 thermal analyzer. Mössbauer spectra were recorded using a Ranger MS-900 spectrometer. A ⁵⁷Co source was used at 293 K. Calibration spectra were taken of 0.0005 in iron foil, and all isomer shifts are referred to the

centre of these spectra. The magnetic susceptibility was determined with a Johnson-Matthey susceptometer devised by D.F. Evans. The electrical conductivity at 298 K was measured with a Super Megohmeter model 170, as previously described [6]. Absorption spectra were recorded using Nujol mulls on a Schimadzu 240 recording spectrophotometer.

3. Results and discussion

3.1. IR spectra of the photo- and thermally-treated polymers 1 and 2

At day light for several days or after heating at 100°C for about 40 h in the dark under nitrogen or in open air, polymer 1 exhibits a noticeable colour change from orange to dark blue. The colour changes gradually from orange to pale green, green, pale blue and dark blue with time and heating. The final blue product is stable in air. However, on raising the temperature to 300°C it converts to a brown product. Also, when a disc of 1 is subjected to a pressure of 5000 kg cm⁻² for 5 h, it shows the same colour change. In the same way, irradiation of 1 at 366 nm for 32 h exhibits similar behaviour as that observed for thermal or pressure treatment, yielding a dark blue complex. The IR spectra of these coloured complexes (Table 1 and Fig. 1) exhibit dramatic changes with respect to those of polymer 1. The IR spectra of the pale green 1a, green 1b and pale blue 1c complexes reveal bands at 2050 and 2110 cm⁻¹ which correspond to ν_{CN} of both iron(II) and iron(III) complexes respectively. The relative intensities of the bands corresponding to the Fe(III)-CN building blocks decrease and suffer a shift to lower frequencies, while those of the bands due to the Fe(II)-

Table I
Vibrational frequencies (cm⁻¹) of polymers 1 and 2 and their coloured complexes 1a–d and 2a,b

Compound								Band assignment
1	1a	1b	1c	1d	2	2a	2b	
—	3425ʷ	3425ᵇ	3430ᵇ	3430ᵇ	3460ᵇ	3420ʷ	—	νH_2O
2990	2990	2990	2980	2990	2990	2990	2980	ν_{asym} CH₃
2900	2905	2900	2910	2905	2900	2905	2900	ν_{asym} CH₃
2850	2850	2840	2830	2835	2840	2830	2830	ν_{sym} CH₃
—	2180ˢ	2180	2180	2180ˢʰ	—	—	2170	νCN
2125ˢ	2115	2110	2105ˢʰ	2100	—	—	—	νCN(Fe³⁺-CN)
2100ˢʰ	—	—	—	—	—	2110ˢʰ	2110ˢʰ	νCN(Fe³⁺-CN)
—	2050	2050ˢᵇ	2055ˢ	2055ˢᵇ	2060s	2060	2060	νCN(Fe²⁺-CN)
—	—	—	—	—	2020s	2020	2040	νCN(Fe²⁺-CN)
—	1620	1620	1625	1630	1630	—	—	δH_2O
1400	1405	1410	1410	1410	1390	1400	1390	δCH₃
1185	1185	1185	1180	1185	1190	1190	1190	δCH₃
780	780	780	782	785	780	780	785	νCH₃
560	560	560	555	560	560	558	560	νSn-C
—	460	460ᵐ	455ᵐ	460ᵇ	450ᵐ	450ʷ	455ʷ	νFe²⁺-CN
410	410ᵐ	410ᵐ	412ʷ	410ˢʰ	—	410ʷ	410ʷ	νFe³⁺-CN

Relative band intensities: s = strong, b = broad, sb = strong broad, m = medium, w = weak and sh = shoulder.

CN building blocks increase with time of heating, pressure or irradiation. In the spectra of **1a–d** a new weak band is observed at 2180 cm^{-1} which may correspond to ν_{CN} of the non-connected cyanide groups whose presence becomes considerable. The existence of this band is further supported by measuring the IR spectra of polymer **1** after heating at 100°C for 10, 30 and 40 h. The IR spectra reveal this band at the same position, while it is not observed in the IR spectrum of Prussian blue. Also, a new band appears at 460 cm^{-1} due to stretching vibrations of the Fe(II)–C bond, while the intensity of the band at 410 cm^{-1} due to $\nu_{Fe(III)-C}$ decreases until it appears as a shoulder in the IR

spectrum of the blue complex **1d**. The coloured complexes retain their polymeric nature through the trimethyltin acting as connecting units; the IR spectra reveal bands due to vibrational modes of the methyl groups at 2990, 2910, 2850, 1410, 1185 and 780 cm^{-1} as well as a ν_{Sn-C} band at 560 cm^{-1} which suffers no change under the effect of heating, pressure or irradiation. In addition, the IR spectra of **1a–d** show the development of a broad band at 3430 cm^{-1} and a medium one at 1620 cm^{-1}, corresponding to the stretching modes of vibration of the water molecules. These bands suggest the presence of water molecules in the coordination sphere of the coloured complexes **1a–d**.
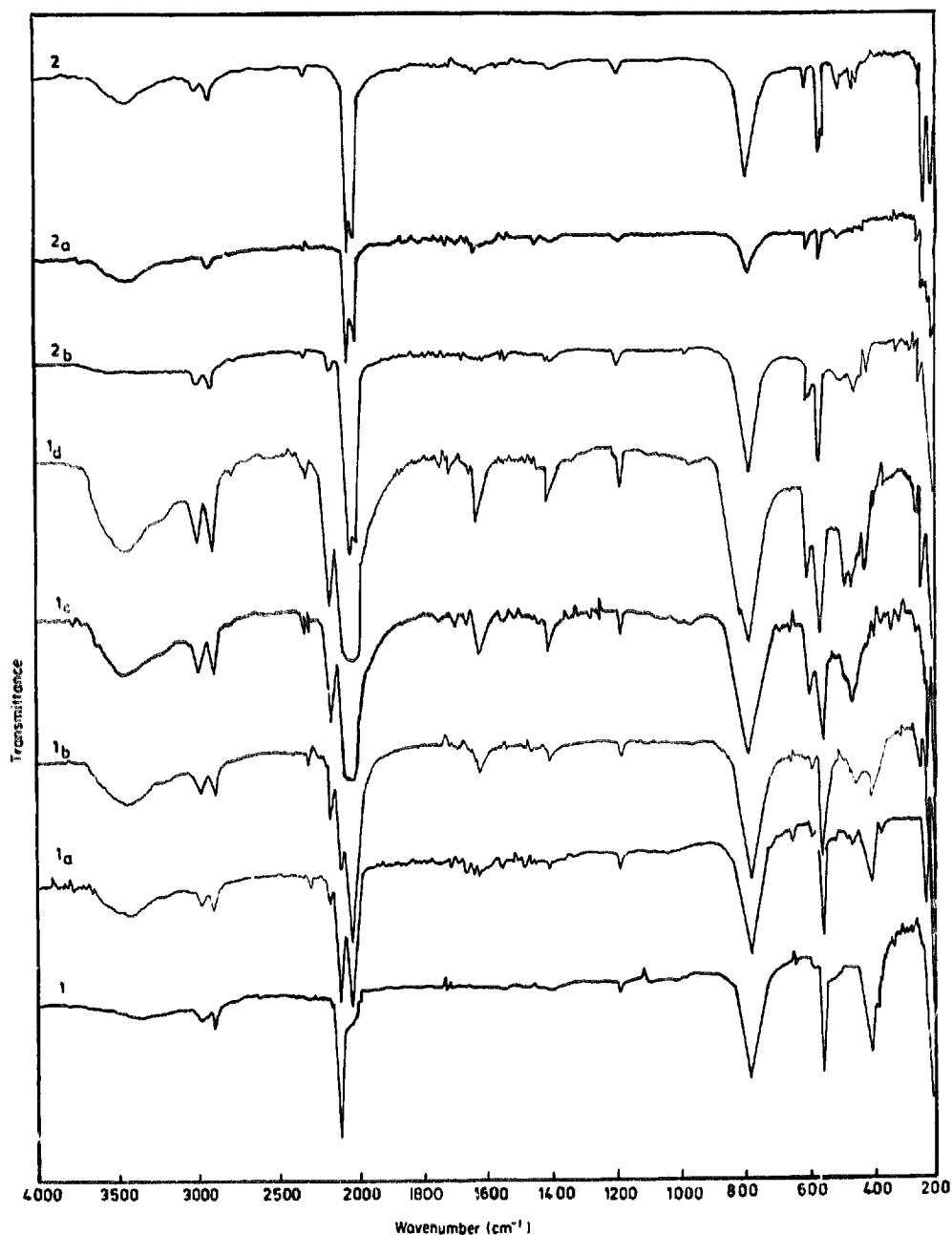

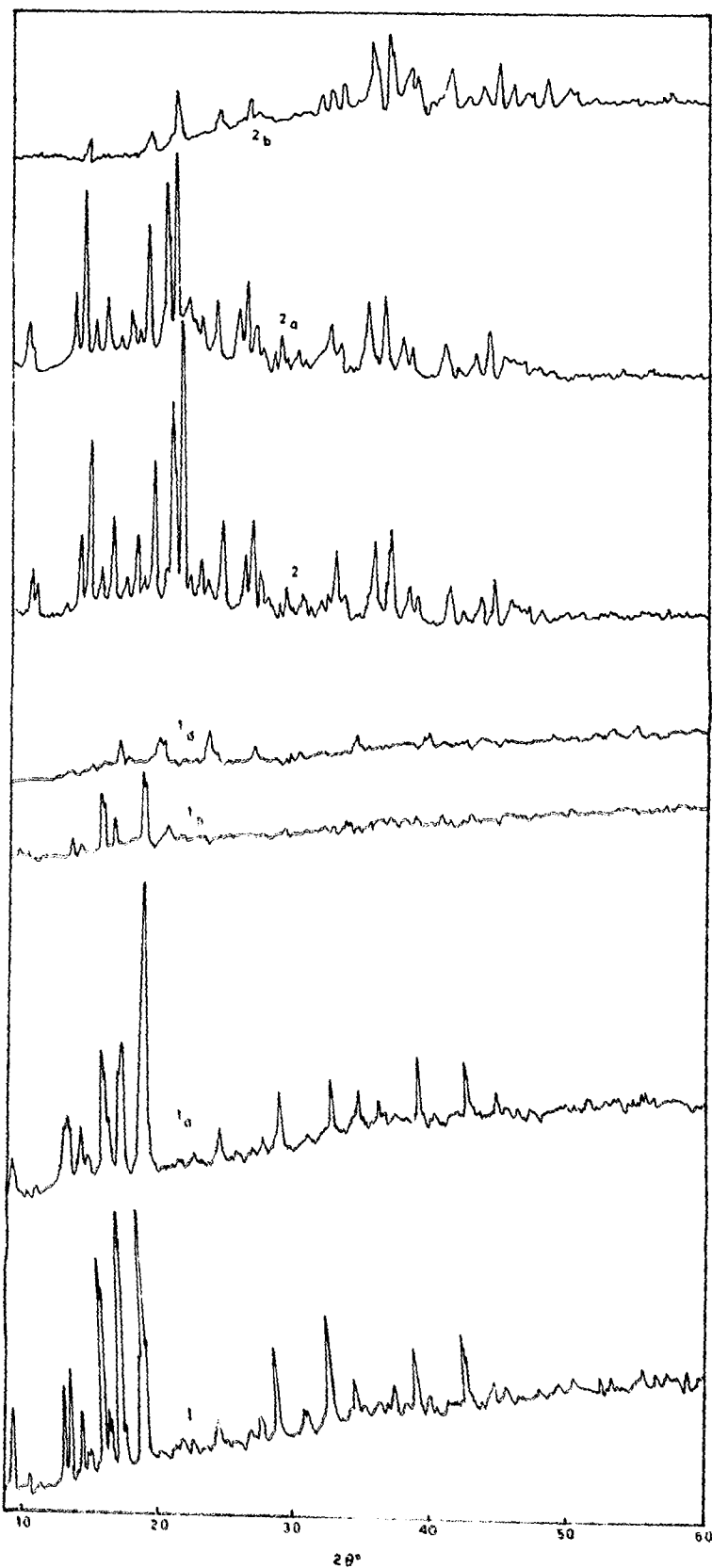Fig. 1. IR spectra of polymers **1** and **2** and their coloured complexes **1a** -d and 2a,b.

Fig. 2. X-ray diffraction of polymers 1 and 2 and their coloured complexes 1a–d and 2a,b.

The polymer 2 is stable on standing in open air at room temperature. However, under the effect of pressure or on heating at 160°C in open air or under nitrogen atmosphere, it turns from white to grey after 20 h, and then to violet after heating for an additional 40 h. On raising the temperature to 300°C, the violet complex is turned to a brown residue, as in the case of polymer 1. The IR spectra of the coloured complexes 2a, b show the original bands of 2 due to the Fe(II)–CN building blocks and bands at 2990, 2900, 2890, 1190, 780 and 560 cm⁻¹ corresponding to the trimethyltin connecting units, in addition to bands at 2110 and 410 cm⁻¹ corresponding to Fe(III)–CN building blocks. Also, the spectrum of 2b exhibits a new band at 2170 cm⁻¹ which resembles that observed in the spectra of 1a–d. In contrast, the IR spectra of the polymer 2 exhibits two bands at 3460 and 1630 cm⁻¹ due to the water molecules of crystallization. These bands disappear in the IR spectra of 2b while a band at 3420 cm⁻¹ appears as a weak broad band in the spectrum of 2a (Table 1 and Fig. 1). Irradiation of polymer 2 at 366 nm for a longe time (ca. 72 h) does not cause any colour changes.

3.2. X-ray powder diffraction

The powder patterns of the polymers 1 and 2 and their coloured complexes 1a–d and 2a,b are given in Fig. 2. On thermal treatment of 1 and 2 or irradiation of 1 at 366 nm the X-ray diffraction lines are broadened and the relative intensities of the original diffraction lines decrease on going from the polymer 1 or 2 to the dark blue or violet complex respectively. In general, the longer the duration of thermal or irradiation treatment of 1 and 2 the more significant the change in diffraction patterns. This indicates a collapse in the crystallinity with keeping the polymeric nature of the complexes, as also gathered from the IR spectra. However, the X-ray

pattern of 2a shows evidence for the formation of a more crystalline form as the diffraction lines shift to lower values. The crystalline form may be formed after loss of water molecules, though the material collapses under the effect of heat or pressure to a less crystalline phase superimposed upon an amorphous phase giving weak broad diffraction lines. This is probably due to small particle size under the effect of heating or pressure, which also makes the determination of the unit cell dimensions rather difficult. Comparing the diffraction patterns of 1, 1b and 2, 2a indicates that they are isomorphous, while those of 1d and 2b are not isomorphous with those of 1 and 2 respectively.

3.3. Thermal analysis

The DTA curve of 1 reveals a weak broad endothermic peak at 67°C corresponding to the release of trace amounts of H_2O. Another two weak exothermic peaks appear at 140 and 165°C, attributed to subsequent release of the cyanide groups (Table 2). In contrast, a strong broad exothermic peak and a broad weak one appear at 239.7°C (temperature range 206–249°C) and 256.3°C (temperature range 249–298°C) respectively, corresponding to major decomposition of the polymeric species due to the release of the (Me_3Sn) connecting units and the cyanide groups, as indicated by the disappearance of the ν_{CN} bands in the IR spectrum of the residue taken at 300°C. This is further supported by the TG curve of polymer 1 (Fig. 3), which indicates the release of one cyanide group (3.8% weight loss) in the temperature range 180–208°C followed by the loss of the (Me_3Sn) connecting group at 208–300°C. The polymer suffers further decomposition at higher temperatures, losing 77% of its weight to give Fe_2O_3. At 609°C a weak broad exothermic peak appears due to complete decomposition of the complex to Fe_2O_3, as indicated by

Table 2
TGA and DTA data and activation energies ΔE^* of decomposition of polymers 1 and 2 and their coloured complexes

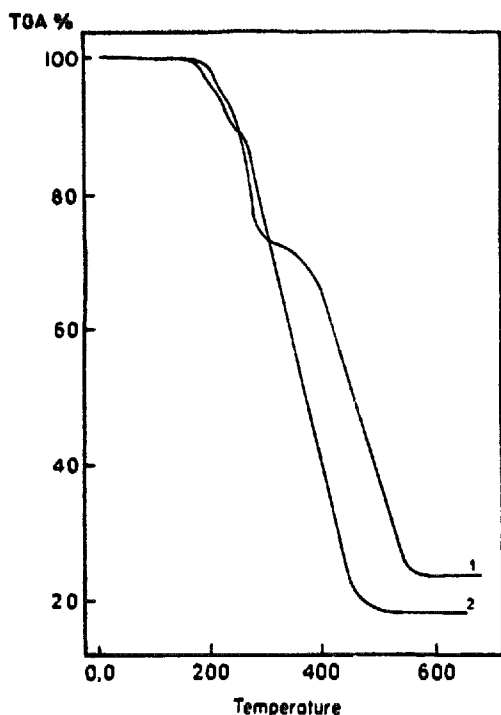| Transitions: temperature range (°C)/ percentage weight loss		Peak (°C)/(ΔE^*)(kJ mol⁻¹)						
		1	1a	1b	1d	2	2a	2b
1	2							
180–208	170–200	67 [#]	78	86 [•]	—	87 [#]	92 [#]	—
3.8	4.0	(134.1)	(130)	(98)	—	(218.7)	(180)	—
208–300	200–230	140	143	—	—	—	—	211 [•]
22.5	5.7	(310.8)	(290.6)	—	—	205	222	259
320–550	255–500	165	181	191	189	(113.9)	(116.2)	(110.5)
50.7	72.3	(245)	(252.3)	(248.6)	(249)	253	275 [•]	—
[•] 180–550	170–500	240	242	253	252	310 [•]	—	—
77.0	82.0	(202.3)	(191.7)	(180.5)	(193)	503 [•]	490 [•]	474 [•]
		256	280	282	291	—	—	—
		609 [•]	574 [•]	591 [•]	593 [•]	—	—	—

[•] Weak broad peak.
[#] Endothermic peak.

Fig. 3. TG curves of polymers 1 and 2.

X-ray powder diffraction, the IR spectrum and iron analysis of the residue. The thermograms of **1a–d** show the development of a new exothermic peak at 181–191°C and the gradual disappearance of the first two exothermic peaks around 78 and 140°C, while the last two exothermic peaks at 181–191°C and 242–253°C exhibit the same behaviour appearing at higher temperatures. The DTA curves of the photo-irradiated derivatives exhibit the same behaviour. The activation energies of the decomposition processes, as calculated by the method of Piloyan et al. [12] (Table 2), show no significant variation on going from polymer **1** to the blue derivative **1d**, (ΔE_a 202.3 and 192.8 kJ mol^{-1} respectively). This reveals that the destruction of the original building pattern causes energetically small effects on the decomposition process.

The DTA curve of polymer **2** exhibits an endothermic peak at 87°C corresponding to loss of water molecules of crystallization. The activation energy of this process is higher than the values reported for similar complexes [13], confirming the increase in crystallinity accompaning the loss of water molecules. A strong exothermic peak appears at 205°C (temperature range 159–212°C) corresponding to the release of (Me₃Sn) guest cations. After that the polymer exhibits stability within the temperature range 212–240°C, followed by further decomposition, losing cyanide groups as indicated by the appearance of two weak exothermic peaks at 253 and 310°C. The IR spectrum of the residue

taken at 300°C does not show the ν_{CN} bands. Also, a weak exothermic peak appears at 503°C, leading to the final decomposition product Fe₂O₃. The TG curve of polymer **2** (Table 2 and Fig. 3) supports the release of the water molecules of crystallization at 170–200°C (4.0% weight loss). This high temperature, relative to that in the case of DTA, is due to the low heating rate (ca. 3.0°C min^{-1}). This step is directly followed by another one at 200–230°C (5.7% weight loss) corresponding to the loss of 31.5% of the (Me₃Sn) guest cations. After that the polymer exhibits thermal stability to about 250°C after which it undergoes complete decomposition, losing 82% of its original weight. The DTA curve of the grey derivative reveals a very weak broad endothermic peak at 92°C which disappears in the DTA curve of **2b**. The DTA curve of **2b** exhibits one weak exothermic peak at 211°C. The strong exothermic peak, corresponding to the release of the (Me₃Sn) guest cations, appears at a higher temperature, while the last exothermic peak, due to complete decomposition, is observed at a lower temperature relative to those of polymer **2**.

3.4. ESR spectra

The room temperature powder ESR spectra of **1** and **2**, as well as of their photo-irradiated or thermally treated derivatives, are complicated and abnormal, making their interpretation rather difficult. The ESR spectrum of **1** shows a complicated fine structure of six g values: 2.05, 2.19, 2.50, 2.95, 3.20 and 4.59 (Fig. 4). These are similar, to some extent, to the behaviour of iron(III) in the strong crystal field of K₃[Fe(CN)₆]; the first three values compare with the g_1, g_2 and g_3 values previously observed in the ESR spectra of K₃[Fe(CN)₆] and some related iron(III) complexes [14–16]. The g values 2.95 and 3.20 correspond to those observed in the ESR spectra of iron(III) complexes with myoglobin imidazole and myoglobin cyanide [17]. These have been attributed to low-spin iron(III), which has a (dE)5 electronic configuration with one unpaired electron in the dyz orbital forming a distorted octahedral structure. The weak signal at 4.59 is known to be characteristic of rhombically distorted high-spin Fe(III) [18,19], and it can be detected even in the case of a trace amount of Fe(III) [20].

After the thermal treatment of **1** at 100°C, leading to a pale green product, dramatic changes in the ESR spectrum are observed, in that only one asymmetric broad signal with g value 3.36 is obtained. It may be resolved into at least three likewise broad signals, those of g values 2.95 and 3.20 corresponding to low-spin iron(III) and that of g value 4.50 corresponding to high-spin iron(III). This broad signal sharpens in the ESR spectrum of the green species **1b** and shifts to lower field ($g = 4.19$). Weak broad signals with g

Table 3

Mössbauer parameters (mm s^{-1}) of polymers 1 and 2 and their coloured complexes 1a–d and 2a,b at room temperature

Compound	δ Fe(III)/Fe(II)	Δ Fe(III)/Fe(II)	w	A
1	−0.31/—	0.228/—	0.41	1.0
1a	−0.59/0.99	0.36/0.0	1.04, 0.71	0.906, 0.094
1b	−0.64/0.87	0.405/0.03	0.89, 1.84	0.83, 0.17
1c	−0.66/1.58	0.39/0.02	1.01, 4.62	0.64, 0.36
1d	−0.65/−0.56	0.37/0.27	1.06, 0.84	0.22, 078
2	—/0.37	—/0.0	0.96	1.0
2a	−0.69/0.41	0.52/0.09	1.04, 1.27	0.23, 0.77
2b	−0.71/0.45	0.46/0.04	0.96, 1.44	0.31, 0.69

δ, Δ, w and A denote the isomer shift, quadrupole splitting, line width and fractional area respectively.

values 2.10 and 2.80 are also observed. Finally, when the sample has been converted into the blue complex 1d, the ESR signal becomes broad again with g value 2.48 while the signal due to high-spin Fe(III) becomes more intense and sharpens with g = 4.19. This behaviour can be attributed to the partial transformation of Fe(III) into Fe(II) leading to the formation of a Prussian blue-like material. However, the ESR spectrum of 2 is typical of the low-spin [Fe^{II}(CN)$_6$]$^{4-}$ ion, which is known to be ESR inactive. The ESR spectrum of 2a exhibits broad signals with g values 4.95, 3.22, 3.05 and 2.08, while the ESR features of 2b are similar to the blue species 1d with one sharp signal (g = 4.16) and one weak broad signal (g = 2.09) (Fig. 4) indicating the partial transformation of Fe(II) into Fe(III).

3.5. Mössbauer spectra

Mössbauer spectra data of polymers 1 and 2 and their coloured complexes, isomer shifts δ, quadrupole splittings Δ, line widths w and fractional areas A$_i$ are listed in Table 3. The data were determined using a computer

curve-fit program and are expressed in millimeters per second. The isomer shift is with respect to the centre of the six-line spectrum of natural iron at 293 K. The Mössbauer spectrum of 1 shows a peak of δ = −0.31 mm s^{-1} and Δ = 0.228 mm s^{-1}. The value of the isomer shift is that expected for low-spin iron(III) [21]. This peak becomes broad with the appearance of another weak broad peak upon thermal treatment or irradiation of polymer 1. These peaks exhibit quadrupole doublets one due to Fe(III)–CN building blocks in the coloured complexes and the other due to Fe(II)– `I building blocks, having a value of 0.27 for complex 1d while for the other complexes the quadrupole splitting is very small, vanishing in experimental errors (Table 3). These Mössbauer data demonstrate clearly that a redox reaction is involved where the Fe(III)–CN building blocks are partially reduced by liberation of cyanide ions under the effect of heat or irradiation. The quadrupole of Fe(III), as shown in Fig. 5a, increases with increasing thermal treatment or irradiation of 1 due to the distortion of the charge distribution around the ^{57}Fe nucleus. In contrast, the increase in absolute value

Table 4

Colour, magnetic susceptibility, electrical conductivity and elemental analysis data of polymers 1 and 2 and their coloured complexes 1a–d and 2a,b

Compound	Colour	Elemental Analysis Calc./(Found)				μ$_{eff}$ BM	σ$_{298 K}$ (Ω^{-1} cm^{-1})
		C	H	N	Fe		
[(Me$_3$Sn)$_3$Fe(CN)$_6$]$_x$ (1)	Orange	25.61 (25.68)	3.86 (4.10)	11.94 (11.32)	7.93 (7.86)	2.18	3.8 × 10^{-8}
{[(Me$_3$Sn)$_3$Fe(CN)$_5$H$_2$O]$_{0.1}$[(Me$_3$Sn)$_3$Fe(CN)$_6$]$_{0.9}$}$_x$ (1a)	Pale green	25.47 (25.50)	3.90 (3.92)	12.95 (12.13)	7.94 (7.91)	2.0	7.9 × 10^{-8}
{[(Me$_3$Sn)$_3$Fe(CN)$_5$H$_2$O]$_{0.17}$[(Me$_3$Sn)$_3$Fe(CN)$_6$]$_{0.83}$}$_x$ (1b)	Green	25.37 (25.32)	3.93 (4.03)	11.63 (10.93)	7.95 (7.96)	1.80	2.3 × 10^{-7}
{[(Me$_3$Sn)$_3$Fe(CN)$_5$H$_2$O]$_{0.36}$[(Me$_3$Sn)$_3$Fe(CN)$_6$]$_{0.64}$}$_x$ (1c)	Pale blue	25.17 (25.20)	3.98 (3.90)	11.27 (10.81)	7.97 (7.95)	1.45	2.5 × 10^{-6}
{[(Me$_3$Sn)$_3$Fe(CN)$_5$H$_2$O]$_{0.78}$[(Me$_3$Sn)$_3$Fe(CN)$_6$]$_{0.22}$} (1d)	Bl	24.49 (24.31)	4.12 (4.08)	10.48 (10.21)	8.01 (7.98)	1.08	3.8 × 10^{-5}
[(Me$_3$Sn)$_4$Fe(CN)$_6$]$_x$ (2)	White	23.93 (23.95)	4.46 (4.45)	9.30 (9.18)	6.18 (6.18)	—	2.3 × 10^{-8}
{[(Me$_3$Sn)$_3$Fe(CN)$_6$]$_{0.23}$[(Me$_3$Sn)$_4$Fe(CN)$_6$]$_{0.77}$}$_x$ (2a)	Grey	25.11 (25.21)	4.10 (4.22)	10.29 (10.18)	6.73 (6.68)	0.40	9.1 × 10^{-8}
{[(Me$_3$Sn)$_3$Fe(CN)$_6$]$_{0.31}$[(Me$_3$Sn)$_4$Fe(CN)$_6$]$_{0.69}$}$_x$ (2b)	Deep violet	25.06 (25.16)	4.12 (4.36)	10.13 (9, 89)	6.84 (6.83)	0.69	1.2 × 10^{-5}

of the isomer shift (Fig. 5b) clears the creation of Fe(II) rather than Fe(III) which changes the charge concentration around ^{57}Fe(III), confirming the redox reaction which leads to the partial transformation of Fe(III) to Fe(II). This behaviour is clear in Fig. 5c, which shows the relative abundance of Fe(III) and Fe(II) in the complex where the concentration of Fe(III) decreases and the concentration of Fe(II) increases under the
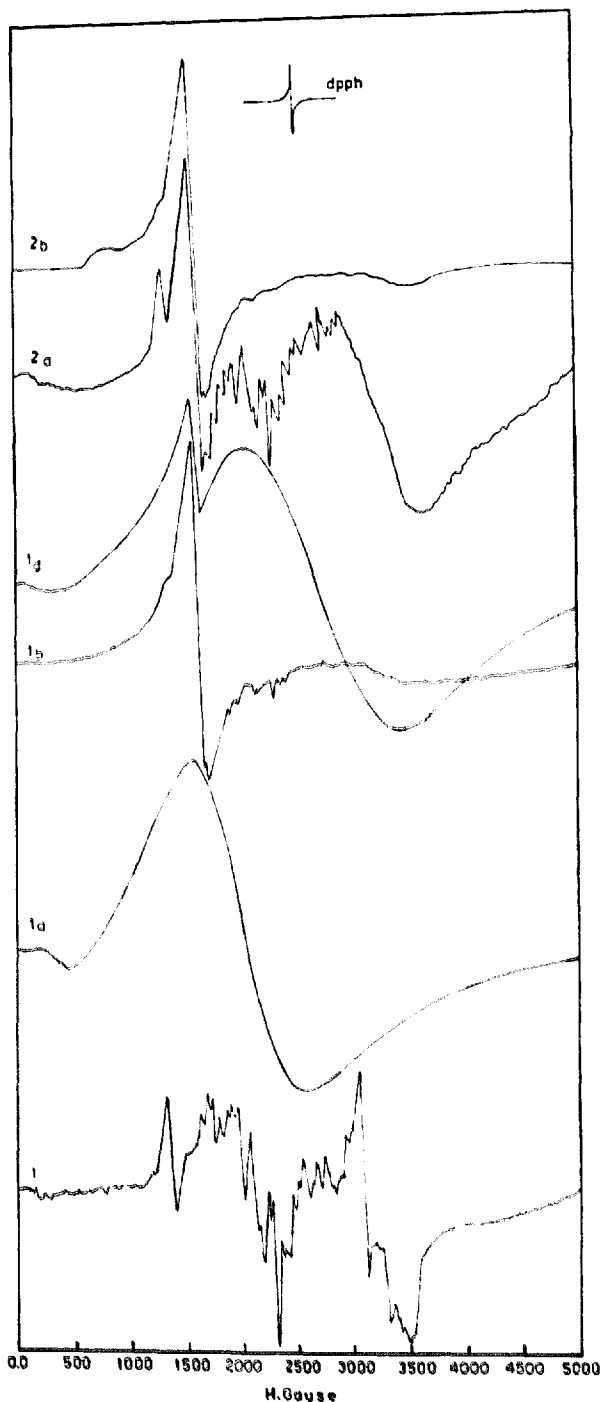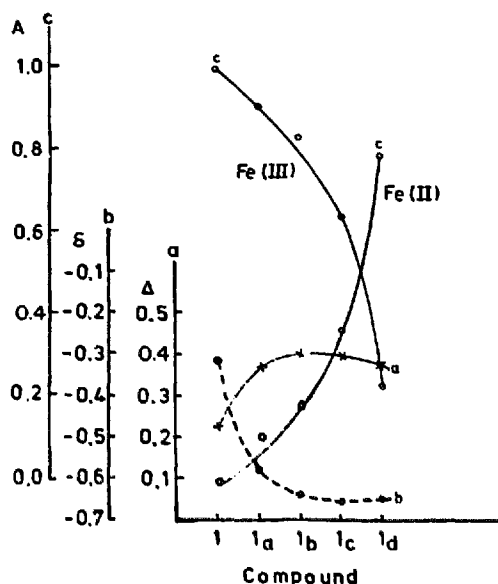

Fig. 5. Quadrupole splitting Δ, isomer shift δ and fractional area A as a function of polymer 1 and its coloured complexes 1a–d, and A as a function of polymer 2.

effect of heating or photo-irradiation. The ratios of Fe(III)/Fe(II) for 1a–d, obtained from Mössbauer spectra (Table 3), support the results of TGA and elemental analysis (cf. Table 4). The Mössbauer spectrum of 2 exhibits one broad band with a weak shoulder of $\delta = 0.37$ mm s^{-1}. The spectra of 2a,b exhibit quadrupole doublets, one due to Fe(III) and the other due to Fe(II) having a very small value, vanishing in experimental errors (Table 3). The spectra reveal the presence of a redox reaction where a fraction of Fe(II) is converted to Fe(III) as indicated by the ratio of Fe(III)/Fe(II). These ratios are in good agreement with the results obtained from TGA and elemental analysis.

3.6. UV and visible spectra

The absorption spectra of the solid matrix of polymers 1 and 2 and their coloured complexes, as well as that of Prussian blue, are shown in Fig. 6. The absorption spectrum of 1 exhibits bands at 230, 295 and 430 nm, while that of 2 reveals two absorption bands at 288 and 320 nm. The bands at the longer wavelength (ca. 430 and 320 nm) correspond to electronic transitions within the Fe(III)–CN and Fe(II)–CN building blocks respectively [6] and they are similar to those observed in the UV spectra of K$_3$[Fe(CN)$_6$] and K$_4$[Fe(CN)$_6$]. The spectra of 1a and 1b have the same features as that of 1, with a decrease in intensity and a small red shift of the band at 430 nm. In contrast, the spectra of 1c and 1d show a new broad band at 620 nm while the intensity of the band at 430 nm decreases dramatically, suffering a blue shift (ca. 400 nm). The absorption spectrum of 2a is more or less similar to that of 2, while the spectrum
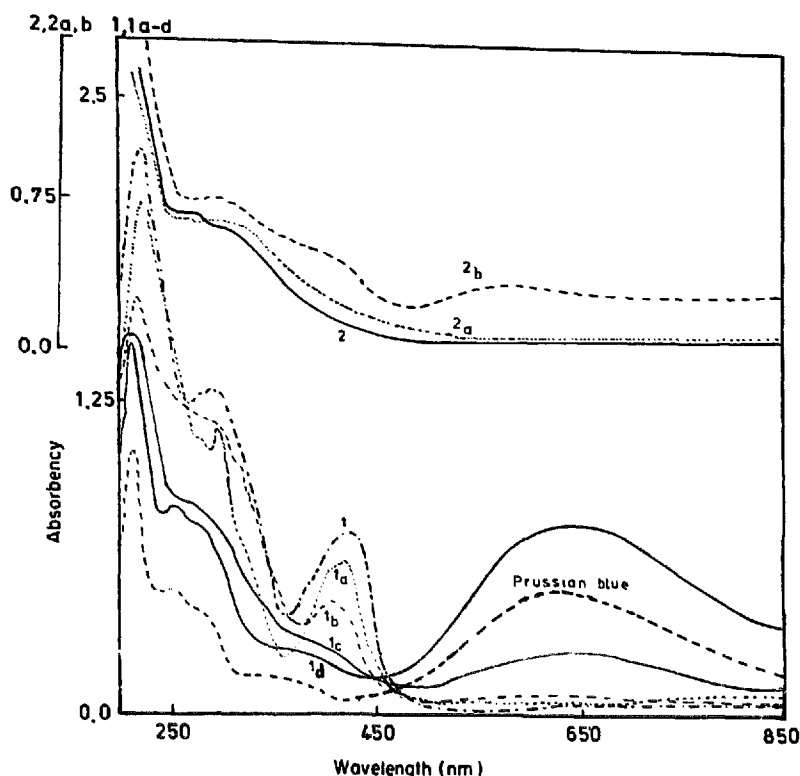

Fig. 4. ESR spectra of polymer 1 and the coloured complexes 1a–d, 2a and 2b.

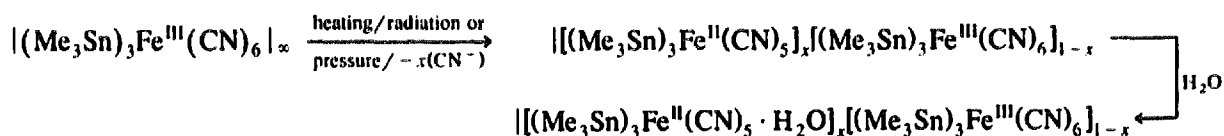Fig. 6. Electronic absorption spectra of the solid matrix of the coloured complexes 1a–d, 2a, 2b and Prussian blue.

of 2b shows a weak band at 390 nm and a broad one at 590 nm. Also, the spectra of the same sample of 1 and 2 under the effect of time or heating show a gradual decrease of the band at 430 nm and the development of a band at 620 nm for 1 and the appearance of a new band at 590 nm for 2. This new band is similar to the band at 620 nm observed in the absorption spectrum of Prussian blue and corresponds to a charge transfer transition between the Fe(II)–CN and Fe(III)–CN building blocks.

4. Conclusion

The foregoing studies indicate that a redox reaction occurs, yielding mixed valence iron polymers on subjecting polymers 1 and 2 to heat and pressure as well as irradiation of 1. The colour of the sample depends on the ratio of Fe(II)–CN/Fe(III)–CN building blocks, as indicated by the Mössbauer spectra. These ratios were confirmed by elemental analysis of the coloured complexes (Table 4). The final products have the same

colour features as Prussian blue. However, they retain a three-dimensional network via the trimethyltin connecting units. The structure of the mixed valence polymers 1a–d and 2a,b was also confirmed by magnetic susceptibility measurements (Table 4) which decrease on going from 1 to 1d and increase from 2 to 2b (the polymer 2 is diamagnetic). The magnetic susceptibilities of 1b, 1c and 2a are in good agreement with Fe(II)/Fe(III) ratios obtained from Mössbauer spectra and elemental analysis, while those of 1d and 2b are higher than expected. However, these low magnetic susceptibilities, relative to that of Prussian blue (ca. 5.97 BM) [22], confirm the presence of mixed valence Fe(II)–CN/Fe(III)–CN building blocks with a very low possibility of the presence of high-spin Fe(III), a case not to be ignored since it could be responsible for the relatively high magnetic susceptibility of 1d and 2b, as also gathered from the ESR spectra.
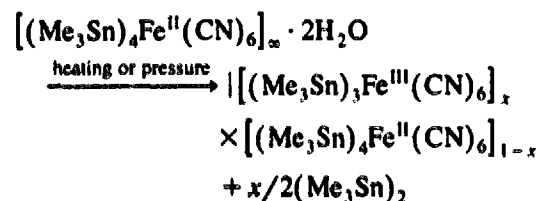
Elemental analysis of 1b–d and TGA of polymer 1 indicate the release of one cyanide ion per molecule from the lattice of the polymer. The cyanide ions reduce Fe(III) to Fe(II) while cyanogen gas is liberated. The colour change can be represented as follows:

$$|(Me_3Sn)_3Fe^{III}(CN)_6|_\infty \xrightarrow[\text{pressure}/-x(CN^-)]{\text{heating/radiation or}} |[(Me_3Sn)_3Fe^{II}(CN)_5]_x[(Me_3Sn)_3Fe^{III}(CN)_6]_{1-x}$$

$$|[(Me_3Sn)_3Fe^{II}(CN)_5 \cdot H_2O]_x[(Me_3Sn)_3Fe^{III}(CN)_6]_{1-x} \xleftarrow{H_2O}$$

This argument was also confirmed by collecting the gas evolved during heating of irradiation of polymer 1 under nitrogen atmosphere, dissolving it in sodium hydroxide solution and treating it with ammonium sulfide then ferric chloride; a red colour was formed according to the following equations:

$$(CN)_2 + 2NaOH \rightarrow NaCN + H_2O + NaOCN$$

$$NaCN + (NH_4)_2S \rightarrow NH_4SCN + NH_4OH + NaOH$$

$$3NH_4SCN + FeCl_3$$

$$\xrightarrow{HCl} 3NH_4Cl + Fe(SCN)_3 \cdot 3H_2O \ (red)$$

As the Fe(II)/Fe(III) ratio increases, the colour changes from pale green, to green, pale blue and blue. The products are polymeric, having three-dimensional networks as long as the trimethyltin units connect the iron–cyanide building blocks. The situation is rather different for polymer 2 where the Fe(II)–CN building blocks are stable towards radiation. However, on heating or subjecting polymer 2 to pressure for a long time, a fraction of the trimethyltin guest cations is released, as indicated by TGA and elemental analysis, while Fe(II) undergoes a redox reaction according to the following equation:

$$[(Me_3Sn)_4Fe^{II}(CN)_6]_\infty \cdot 2H_2O$$

$$\xrightarrow{heating \ or \ pressure} |[(Me_3Sn)_3Fe^{III}(CN)_6]_x$$

$$\times [(Me_3Sn)_4Fe^{II}(CN)_6]_{1-x}$$

$$+ x/2(Me_3Sn)_2$$

The fraction of trimethyltin guest cations is reduced to the corresponding radicals which could undergo dimerization to produce $(Me_3Sn)_2$.

The charge transfer character present in these complexes reflects the behaviour of 1c, 1d and 2b as semiconductors in spite of 1 and 2 being insulators (Table 4). Generally, the electrical conductivity increases as the mixed valence Fe(II)/Fe(III) ratio increases in the case of 1 and decreases in the case of 2. The electronic conductivity of 1d and 2b is quite similar to that observed in Prussian blue-like materials [23]. The actual electrical conductivity is dependent on charge transfer interactions between Fe(III)–CN and Fe(II)–CN building blocks, reflecting the stoichiometry and degree of mixed valence of the system.

References

[1] M. Hassanein and S.H. Etaiw, Eur. Polym. J., 29(1) (1993) 47.
[2] S. Eller, P. Brandt, A.K. Brimah, P. Schwarz and R.D. Fischer, Angew. Chem., Int. Ed. Engl., 28 (1989) 1263.
[3] M. Adam, A.K. Brimah, X.F. Li and R.D. Fischer, Inorg. Chem., 29 (1990) 1595.
[4] S.H. Etaiw and A.M.A. Ibrahim, J. Organomet. Chem., 456 (1993) 229.
[5] S.H. Etaiw and A.M.A. Ibrahim, Thermochim. Acta, 233 (1994) 297.
[6] A.M.A. Ibrahim, T.M. Soliman, S.H. Etaiw and R.D. Fischer, J. Organomet. Chem., 468 (1994) 93.
[7] P. Brandt, A.K. Brimah and R.D. Fischer, Angew. Chem., Int. Ed. Engl., 27 (1988) 1521.
[8] U. Behrens, A.K. Brimah, T.M. Soliman, R.D. Fischer, D.C. Apperley, N.A. Davies and R.K. Harris, Organometallics, 11 (1992) 1718.
[9] D.C. Aperley, N.A. Davies, R.K. Harris, A.K. Brimah, S. Eller and R.D. Fischer, Organometallics, 9 (1990) 2672.
[10] S. Eller, P. Schwarz, A.K. Brimah, R.D. Fischer, D.C. Apperley, N.A. Davies and R.K. Harris, Organometallics, 12 (1993) 3232.
[11] K. Yünlü, N. Höck and R.D. Fischer, Angew. Chem., Int. Ed. Engl., 24 (1985) 879.
[12] G.O. Piloyan, I.D. Ryabchikov and O.S. Novikova, Nature, (1966) 1229.
[13] A. Bonardi, C. Corini, C. Pelizzi, G. Pelizzi, G. Predieri, P. Tarasconi, M.A. Zoroddu and K.C. Molloy, J. Organomet. Chem., 401 (1991) 283.
[14] J.M. Baker, B. Bleaney and K.D. Bowers, Proc. Roy. Soc., 69 (1956) 1205.
[15] Y. Nishida, S. Oshio and S. Kida, Inorg. Chim. Acta, 23 (1977) 59.
[16] P. Beardwood and F.I. Gibson, J. Chem. Soc., Dalton Trans., 4 (1983) 737.
[17] H. Hori, Biochim. Biophys. Acta, 251 (1971) 227.
[18] J. Peisach, W.E. Blumberg, E.T. Lode and M.I. Coon, J. Biol. Chem., 246 (1971) 5877.
[19] S.A. Cotton and J.F. Gibson, J. Chem. Soc. A, (1971) 803.
[20] R. Aasa, S.P.J. Albracht, K.E. Falk, B. Lanne and T. Vanngaed, Biochim. Biophys. Acta, 422 (1976) 260.
[21] P.G. Rasmussen and E.A. Meyers, Polyhedron, 3(2) (1984) 183.
[22] R.E. Wilde, S.N. Ghosh and B.J. Marshall, Inorg. Chem., 9(11) (1970) 2512.
[23] (a) P. Day and A. Ludi, in D.B. Brown (ed.), Mixed-Valence Compounds, Theory and Application in Chemistry, Physics, Geology and Biology, NATO Adv. Study Inst. Ser. 58C, Reidel, Dordrecht, Netherlands, 1980; (b) M.B. Robin and P. Day, Adv. Inorg. Chem. Radiochem., 10 (1967) 247.